Improved Surface Functionalization and Characterization of Membrane Targeted Semiconductor Voltage Nanosensors

Joonhyuck Park[1], Yung Kuo[1], Jack Li[1], Yi-Lin Huang[2], Evan Miller[2], and Shimon Weiss[1,3,4,5]

[1] Department of Chemistry and Biochemistry, University of California Los Angeles, Los Angeles, CA 90095
[2] Departments of Chemistry, and Molecular & Cell Biology, and Helen Wills Neuroscience Institute, University of California Berkeley, Berkeley, CA 94720
[3] California NanoSystems Institute, University of California Los Angeles, Los Angeles, CA 90095
[4] Department of Physiology, University of California Los Angeles, Los Angeles, CA 90095
[5] Department of Physics, Institute for Nanotechnology and Advanced Materials, Bar-Ilan University, Ramat-Gan, 52900, Israel

Abstract

Type-II ZnSe/CdS voltage sensing seeded nanorods (vsNRs) were functionalized with alpha-helical peptides and zwitterionic decorated lipoic acids (zw-LA). Specific membrane targeting with high loading efficiency and minimal non-specific binding was achieved. These vsNRs display quantum yield (QY) modulation as function of membrane potential (MP) changes, as demonstrated at the ensemble level for (i) vesicles treated with valinomycin and (ii) wild type HEK cells under alternating buffers with different [K^+]. ΔF/F of ~ 1% was achieved.

TOC entry:

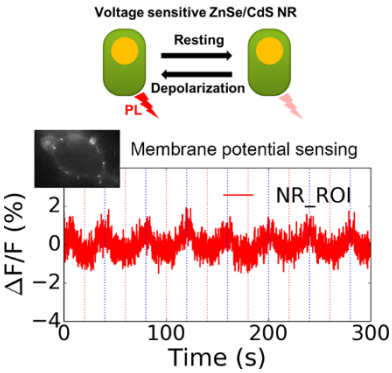

The complex and temporal dynamics in brain systems has been difficult to understand and unravel. In order to untangle the brain activity, tools which allow to record and interpret the interactions between individual neurons simultaneously are needed to develop. Measuring the electrical activity of large neuron populations in brain tissue with high spatial and temporal resolution is crucial to comprehend the dynamics. Numerous technologies for the cell membrane potential recording have been developed for decades.

Voltage-sensitive dyes (VSDs) could potentially allow to visualize the neuronal activity simultaneously over a large number of neurons in a large field-of-view and afford direct imaging of the membrane potential in mammalian brain slices and whole brains of awake mammals.[1-3] However, VSDs could alter membrane capacitance, be phototoxic and suffer from photo-bleaching, short retention time in the membrane.[4] Recently, several genetically-encoded voltage indicators (GEVIs) have been developed to detect aggregate neural activity in vivo and single action potential in brain tissue level using their fast response kinetics and red emission profile.[5-8] Other types of voltage sensitive nanoparticles (VSNs) were also reported. Rowland and coworkers elucidated the electric field-driven QD ionization and quasi-type II QD PL quenching.[9] C60-quantum dots (QDs) conjugates, modulating their PL by changing of the Foster energy resonance transfer (FRET) efficiency between C60 quenchers and QD, were also developed by Nag et al.[10] We previously demonstrated the voltage sensitive quasi-type II CdSe/CdS nanorods (NRs) at room temperature and single particle level.[11] We have theoretically evaluated their potential utilization as membrane voltage sensors and examined modes of detections based on intensity changes ($\Delta F/F$), spectral shifts ($\Delta\lambda$), and excited-state lifetime changes ($\Delta\tau$).[12] We showed that when functionalized with trans-membrane peptides, voltage-sensing nanorods (vsNRs) can be inserted into cellular membranes to report the

membrane potential[13] via fluorescence intensity or spectral changes. More recently, we have shown that type-II ZnSe/CdS seeded nanorods (CdS nanorods while embedding the ZnSe QDs inside, same composition NRs in this paper) exhibit the largest quantum-confined Stark effect (QCSE) among a small library of different compositions and shapes nanoparticles. However, we also observed positive correlation between spectral shift ($\Delta\lambda$) and PL changes ($\Delta F/F$), in disagreement with usual QCSE predictions, for type-II ZnSe/CdS seeded nanorods[14]. We assumed that extrinsic charging/ionization at surface defects of nanorods could possibly modulate blinking rates (and hence QY) and contribute to the positive $\Delta\lambda$-$\Delta F/F$ correlation. The QCSE could be directly monitored by $\Delta\lambda$ measurements, but $\Delta F/F$ measurements were also affected by extrinsic effects, most likely via quantum yield (QY) modulation due to charging and/or ionization at surface- and interface- defects.[14-16]

Here we further developed and examined voltage sensing nanorods (vsNRs) while focusing on QY modulation (due to charging). These vsNRs could offer unique advantages for sensing the membrane potential: (i) they are very bright and could, in principle, afford single-particle detection; (ii) they display modulated QY as function of voltage change across cell membrane, which presumably is originated by charging on surface's defect; (iii) with an improved surface coating composed of a mixture of alpha-helical peptides and zwitterionic decorated lipoic acids (zw-LA), they could target the cell membrane with high loading efficiency and minimal non-specific binding. The mixture of peptides and zw-LAs, which contain both positive and negative charges over wide pH range, provide better colloidal stability to the nanoparticles and decreased non-specific adsorption as compared to peptide-only coating[13].

ZnSe/CdS type-II semiconductor nanorods(NRs) were synthesized by the heat-up

method.[17] Briefly, premade ZnSe quantum dots (QDs) were mixed into a solution of cadmium phosphonates and octadecanethiol (cadmium and sulfur precursors). The phosphonic acids in the mixture promote the anisotropic growth of CdS nanorods while embedding the ZnSe QDs inside ('seeded NRs').[17] The mixture was heated up to ~320 ^{o}C for 15 minutes to grow NRs and cooled to room temperature (r.t.) yielding NRs of 11.8±2.3 nm in length and 6.5±1.5 nm in diameter (# of nanorods for the measurement=50).

To deliver NRs to cell membranes, we improved the previously reported peptide-coating approach.[13] In addition to the modified alpha-helical trans-membrane peptides, we also added zwitterionic decorated lipoic acids (zw-LA)[18] to provide colloidal stability. Ligand exchange reaction of the mixture was performed through multiple steps (See Methods section for detail). Briefly, as-synthesized NRs (asNRs) were first treated with the ligand stripping agent (triethyloxonium tetrafluoroborate) to remove the original hydrophobic ligands[19], such as alkylphosphonic acids, alkylphosphine oxides or alkylamines on the surface of NRs. IR spectroscopy was used to monitor the ligand stripping efficiency. As can be seen in Fig. S1, the C-H vibration (2852, 2922 cm^{-1}) and the bending peaks (1466 cm^{-1}) were diminished after the stripping treatment. Next, octanoic acid was added to the NRs solution to provide temporal colloidal stability. After removing excess amount of octanoic acid, pyridine was added (acting both as a surface

ligand and as a solvent). Pyridine capped NRs were then mixed with the mixture of 1:3 of zw-LA : alpha-helical peptides and redispersed in DMSO. The optical properties of these zw-LA-and-peptides (ZAP) functionalized NRs were preserved after the ligand exchange process as characterized by UV-Vis absorption and fluorescence spectroscopy (emission peak: 605 nm, Figure 1a). The quantum yield (QY) of the functionalized ZAP-NRs was only slightly reduced (to 39%) as compared to the original QY of the asNRs (55%). Transmission electron microscopy (TEM) images of the asNRs and the ZAP-NRs showed no substantial change in size after functionalization (Figure 1b, c, long axis = 11.8±2.3 nm and short axis = 6.5±1.5 nm for asNRs, long axis = 12.0±2.4 nm and short axis = 6.7±1.9 nm for ZAP-NRs (# of nanorods for the measurement=50)). The 1:3 ratio of zw-LAs to alpha-helical peptides was chosen since it was able to provide both colloidal stability and membrane loading efficiency. This ratio is similar to the previously reported primary amine functionalized ligands to zw-LAs ratio used to minimize non-specific adsorption.[18]

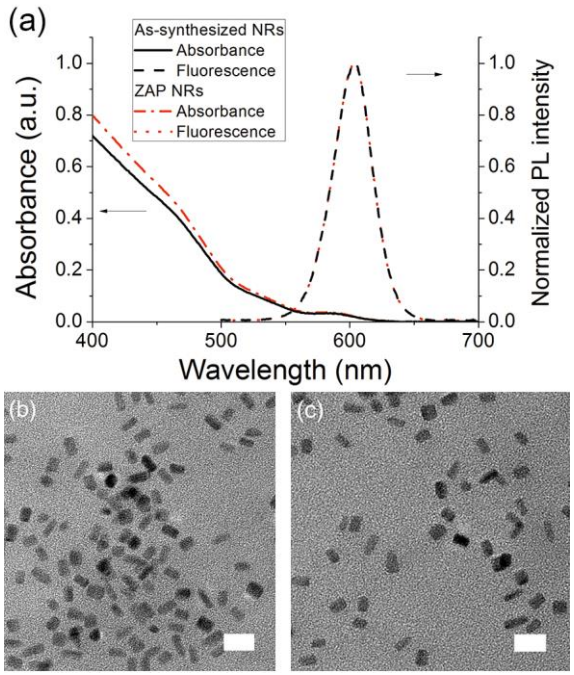

Fig. 1: (a) Absorption (black solid) and fluorescence (red dash-dotted) spectra of as-synthesized (black dashed) and ZAP-NRs (red dotted). TEM images of (b) as-synthesized ZnSe/CdS nanorods and (c) ZAP-NRs (scale bar: 20 nm).

Interestingly, ZAP-NRs were colloidally stable at 10% and down to 1% DMSO(aq) but started to form aggregates at 0.2% DMSO(aq) as shown by DLS measurements (Fig. 2e). Zeta potential of ZAP NRs was slightly negative (-13.2±2.2 mV at 1% DMSO

condition, # of measurement=10, Fig. S2), attesting to their solubility and colloidal stability. We argue that the amphiphilic nature of the peptides affords the dispersion of ZAP-NRs in DMSO, while the zw-LAs afford their partial solubilization in DI water (Fig. S3).

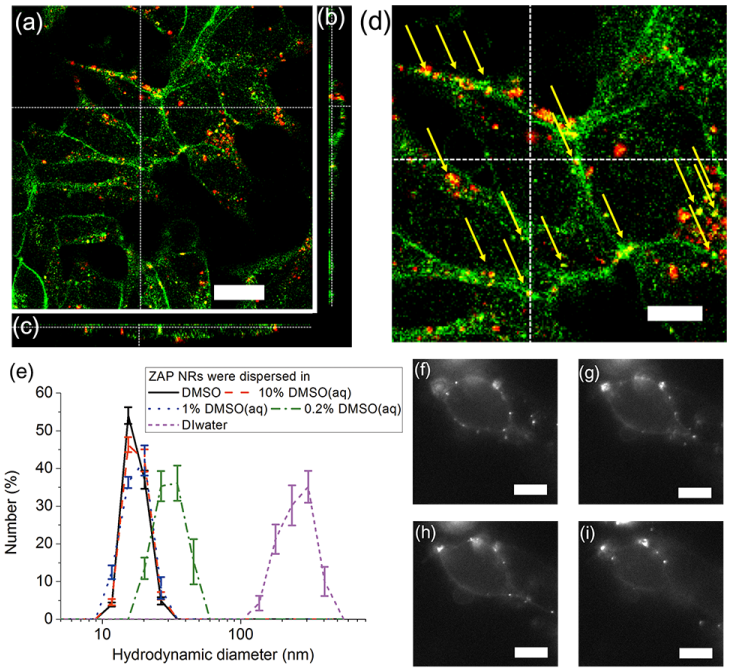

Fig. 2: (a) Confocal microscope image of both ZAP-NRs (red) and DiR dye (green) labeled HEK293T cells (scale bar: 20 μm). Cross-section images of (b) yz and (c) xz plane through the white dotted line in (b). (d) Yellow arrows indicated colocalized ZAP NRs (yellow signals) with membrane labeling dyes (green signals) (scale bar: 10 μm). (e) DLS-derived hydrodynamic diameters of ZAP-NRs in: DMSO (black solid), 10% DMSO(aq) (red dashed), 1% DMSO(aq) (blue dotted), 0.2% DMSO(aq) (green dash-dotted), DI water (violet short dashed). (f-i) Wide-field fluorescence images of ZAP-NRs labeled HEK293T cells at different heights from the focal plane (scale bar: 10 μm).

Membrane loading ability and specificity of ZAP-NRs were assessed by confocal microscopy (Figs. 2b-d). HEK293T cells were sequentially incubated with 30 nM ZAP-NRs for 1 hour (the mean PL intensity from ZAP-NRs labeled HEK cells were saturated after 1 hour, FACS data with different incubation time in Fig. S4) and then with 2 μM DiR membrane staining dye for 15 minutes. Next, cells were fixed with 4% paraformaldehyde for 15 minutes at r.t..

At the diffraction-limited resolution of the confocal microscope, ZAP-NRs (red channel) and DiR dye (green channel) seem to be co-localized at the cell membrane (Fig. 2a and a zoom-in Fig. 2d), as supported by *y-z* and *x-z* cross-section images (Figs. 2b, 2c) through the yz- or xz-planes. Yellow arrows in Fig. 2d showed the co-localized ZAP-NRs with membrane, and some of them (red dots) were internalized into HEK cells. Wide-

field fluorescence images at different focal planes also support co-localization (Figs. 2f-i). At the edge of HEK cells, which would be cell membrane mainly, there were smaller single ZAP-NRs and also some of aggregated ZAP-NRs after their intracellular delivery. We think that these aggregates would not be sensitive under membrane potential and doesn't affect the voltage sensitivity of membrane labeled ZAP NRs.

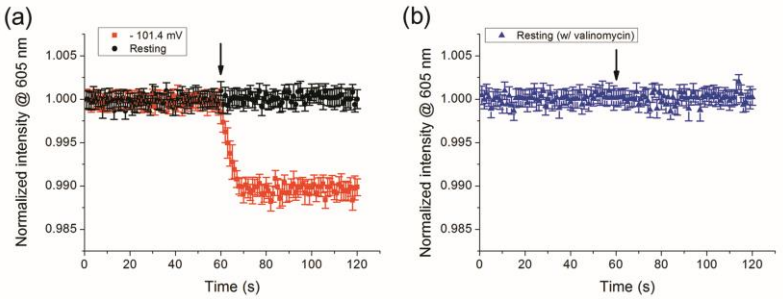

Fig. 3: (a) Time-lapse PL intensity measurement of ZAP-NRs labeled vesicles (a) under membrane potential of -101.4 mV (with $[K^+]$=2.7 mM outside and $[K^+]$=140 mM inside of the vesicle, red square). This potential was abolished at t=60 sec after valinomycin addition (arrow). If valinomycin is not added, there is no change in the membrane potential (black circle). (b) Control experiment (blue triangle): time-lapse PL intensity measurement of ZAP-NRs labeled vesicle under resting conditions, with $[K^+]$=2.7 mM outside and inside of the vesicle; valinomycin was added at t=60 sec (arrow).

We were able to observe the ZAP-NRs associated with the membrane after 1 hour incubation, while negatively- or positively-charged QDs were internalized much faster under similar conditions.[18] We note, however, that these observations only report on the association of ZAP-NRs to membranes; they do not provide evidence for membrane insertion. Nonetheless, functional assays (reported below) do suggest that at least some portion of the ZAP-NRs are inserted into the membrane.

To assess voltage sensitivity (at the ensemble level), ZAP-NRs were loaded into lipid vesicles prepared in a HEPES buffer (20 mM, pH 7.4) with $[K^+]$=140 mM and then placed into a isosmotic HEPES buffer (20 mM, pH 7.4) with $[K^+]$=2.7 mM. This preparation establishes a potential of -101.4 mV (as determined by the Nernst equation) across the membrane. Valinomycin, a naturally occurring potassium ionophore (extracted from Streptomyces cells) was added at t=60sec to the vesicles. Once valinomycin was

introduced, K^+ ions flowed (from inside to outside of the vesicles) to equalize the [K^+] concentration gradient, thus abolishing the established membrane potential.[20] Vesicle membrane labeling by ZAP-NRs was confirmed by fluorescence microscopy (Fig. S5). The ZAP-NRs photoluminescence (PL) intensity was monitored at 605 nm for 120 sec during this process (Figs. 3a, S5). Valinomycin was added at t=60 sec. A clear drop in ZAP-NRs' PL is seen at this time point (red curve), from which we could calculate $\Delta F/F = 1.1\pm0.2$ % per 100 mV (# of sample=5, p-value was 0.005 (statistically significant) with t-test under the comparison between no valinomycin treated sample). Here, ΔF was defined as the difference between the PL intensity at 605 nm from the sample before and after valinomycin treated. F was defined as the PL intensity at 605 nm from the sample before valinomycin treated. The control experiments (no valinomycin added in same buffer condition (Figs. 3a, black circle) or no established membrane potential – by having the same [K^+]=2.7 mM inside and outside of the vesicle – with valinomycin (Figs. 3b, blue circle)) show no change in PL intensity (black and blue curves respectively, Figs. 3a,b). When a full PL spectrum of the ZAP-NRs was recorded, a similar drop of 1% was observed after the addition of valinomycin (Fig. S6).

Monitoring PL changes as function of time also allowed us to monitor the time it takes to establish the resting potential after the introduction of the [K^+]=140 mM vesicles into the [K^+]=2.7 mM buffer. The time for balancing the K^+ ion concentration between

inside and outside of the vesicle was determined to be 9 secs. This time constant is mainly governed by K^+ ion transfer rate through the ionophore. The drop in PL intensity around t=60 secs (Fig. 3a, after the addition of valinomycin) can be governed by the mixing/diffusion of valinomycin, binding constant of valinomycin to the membrane, and the K^+ ion transfer rate through the ionophore. A previous work reported 25 seconds for balancing the difference of [K^+] between inside and outside of a human red blood cell membrane in the presence of valinomycin.[21] We note that PL quenching results for a quasi-type II QDs in PMMA matrix placed between electrodes and subjected to a synthetic voltage sweep of 20 mV yielded ΔF/F as ~2% from the other's published work.[9] However, the actual field strength in this work could be quite different as compared to our experiment due to differences in local environments.

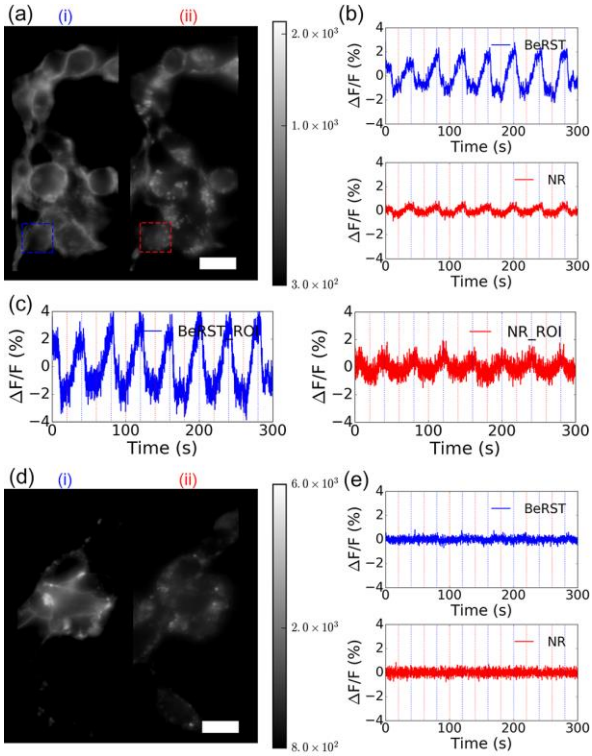

Fig. 4: Chemical modulation of membrane potential of live HEK293T cells. (a) Dual-channel fluorescence microscope images of labeled live HEK293T cells after the addition of valinomycin for (i) the voltage sensitive BeRST dye channel and for (ii) the ZAP-NRs channel. (d) Dual-channel fluorescence microscope images of labeled fixed HEK293T cells for (i) BeRST channel and for (ii) ZAP-NRs channel. (b) and (e) show ΔF(t)/F for the sum ('ensemble average') of all pixels above a threshold (see method) for BeRST (blue) and ZAP-NRs (red) from (a) and (d) respectively. (c) show ΔF(t)/F from certain region of interest (one of HEK293T cells) for BeRST (blue) and ZAP-NRs (red) from dotted-area (blue dotted area: BeRST, red dotted area: ZAP NRs in (a)). Blue or red dotted vertical lines indicate time points for either [K^+]=2.7 mM and [K^+]=140 mM buffer alternation (every 20 seconds, starting with [K^+]=2.7 mM at time = 0 s). Scale bar: 20 μm

To evaluate the membrane potential sensitivity of ZAP-NRs under periodic membrane potential modulation, we pre-cultured HEK293T cells in a flow chamber, loaded ZAP-NRs, and recorded PL changes under periodic buffer exchange (of HEPES

buffers containing either $[K^+]$=2.7 mM or $[K^+]$=140 mM, every 20 seconds, for 7 cycles). This chemical modulation method establishes cell membrane potential modulation in the presence of valinomycin.[21, 22] HEK293T cells were cultured in poly-L-lysine pretreated flow chambers with 6 channels. Cells were first treated with 5 μM of valinomycin for 5 minutes. 1 μL ZAP-NRs (3 μM stock, final concentration would be 30 nM) were then added to the culture medium of each chamber and incubated for 15 minutes. To confirm and calibrate the chemical voltage induction in live HEK293T cells, near infrared (NIR) voltage sensitive dye BeRST[23] (final concentration would be 200 nM) were added to the cells and incubated for 15 minutes. After each labeling step, excess of ZAP-NRs and dyes was removed by a washing step with Dulbecco Modified Eagle Medium (DMEM) growth media (with 10% fetal bovine serum). Control samples were fixed with 4% paraformaldehyde for 10 minutes at room temperature (which disturbs the integrity of cell membrane and abolishes its membrane potential).

The flow chamber was placed on an inverted fluorescence microscope and connected to an automated controlled flow setup. The high ($[K^+]$ = 140 mM) and low ($[K^+]$ = 2.7 mM) concentrations of potassium buffers were continuously alternated every 20 seconds while a dual-view (for both BeRST and ZAP-NRs channels) movie was acquired for a duration of 300 seconds. The excitation intensity was adjusted to 0.2 mW/cm^2 in front of the objective lens. The frame rate was 10 Hz. The slow rise of the signal during each period (~10 seconds) is likely due to K^+ ion transfer rate through the ionophore after buffer exchange (denoted by dotted red or blue lines in Fig. 4b, 4c, and 4e, overlay graphs of BeRST/ZAP NRs signals in Fig. S7). As we mentioned before, a previous report cites a similar 25 seconds to balance the difference of $[K^+]$ between inside and outside of human red blood cell membrane.[21]

An ‘ensemble level’ ΔF/F was calculated from the movie in the following way: First, all pixels above a threshold (Fig. S8) per single frame were averaged. This quantity was then averaged over all frames (time points) to yield F. Next, ΔF was defined as the difference between the averaged intensity over all pixels for a single frame (for each time point) and F. The definition of standard error of the mean (SEM) was standard deviation of mean values from ΔF/F values in same sample group. For the statistics of the chemically modulated experiment in Figure 4, p-value was 0.007 for ZAP-NRs channel and 0.006 for BeRST channel with t-test (comparison with fixed HEK293T cells sample for each channel, Figure S9), which is statistically significant, and sample numbers were 20 in all cases. This operation was performed for each spectral channel, yielding ΔF/F=3.5±0.3 % for BeRST and ΔF/F(±SEM)=1.0±0.2 % for ZAP-NRs per ~200 mV (Fig. 4b). The signal-to-noise ratio was defined as the ratio of peak ΔF/F value over 7 cycles from the sample to the noise level from baseline of ΔF/F from same sample (Fig. 4e). The ΔF/F cited above were obtained for signal-to-noise ratios of ~11 and ~5 respectively, and for a membrane potential sweep of -101.4 mV to +101.4 mV (as determined by the Nernst equation). In terms of absolute brightness, QY of BeRST in TBS/SDS buffer was 2% and QY of ZAP-NRs in PBS buffer was 33%. Since the filter setups we were using for either ZAP-NRs or BeRST were different and their brightness under the microscope images can be determined by their concentration, we note that their QY cannot be extracted directly from the microscope images using our customized setup. To get the signal from a HEK293T cell, ΔF/F operation from certain region of interest (ROI, blue dotted area for BeRST channel and red dotted area for ZAP-NR channel in Fig. 4a) was performed, yielding ΔF/F=4.9±0.5 % for BeRST and ΔF/F=1.8±0.5 % for ZAP-NRs (Fig. 4c). As the absolute value of ΔF/F from the ROI of dual-labeled

HEK293T cells under voltage sweep increased, the standard deviation of ΔF/F was also increased. Several control experiments were performed in order to validate the above result: (i) the same experiment ($[K^+]$ modulation) was performed for ZAP-NRs labeled, and valinomycin pretreated, HEK293T cells after fixation (with 4% paraformaldehyde solution in r.t. for 10 minutes). Fixation disturbed the integrity of membrane and abolishes its membrane potential. Indeed, no signal modulation was observed for fixed cells (Fig. 4d and 4e). This control eliminates the possibility that the signal originates from direct photophysical property change due to the $[K^+]$ modulation itself, but it rather due to the membrane potential modulation; (ii) the same experiment ($[K^+]$ modulation) was performed for either ZAP-NRs-only or BeRST-only labeled live valinomycin pretreated HEK293T cells to eliminate the possibility that the ZAP-NRs signal (in doubly-labeled cells) originates from the BeRST signal (Fig. S9); (iii) the same experiment ($[K^+]$ modulation) was performed for Di-8-ANEPPS-labeled valinomycin pretreated live HEK293T cells. Di-8-ANEPPS is a well characterized and calibrated commercially available voltage sensitive dye (VSD), demonstrating similar PL modulation upon $[K^+]$ modulation for cells treated with valinomycin (Fig. S10). As voltage applied, ΔF/F for Di-8-ANEPPS would decreased in a conventional setup, whereas ΔF/F for BeRST increased.[24-26] However, since we optimized the dichroic cut-off for ZAP-NRs spectra, and not for Di-8-ANEPPS, the observed ΔF/F for the latter was 2.1±0.4 % (p-value was 0.005 with t-test (comparison with fixed HEK293T cells sample, Figure S9)), which is statistically significant, and sample numbers were 10); (iv) Solution-based (*in vitro*) PL measurements of ZAP-NRs as function of $[K^+]$ (in the range $[K^+]$=0.5 mM to $[K^+]$=200 mM) and pH (in the range pH=5 to pH=10) were performed. No significant PL changes were observed (Fig. S11a and S11b); (v) Experiments with no $[K^+]$ modulation was

performed on live HEK293T cells treated with valinomycin and doubly labeled with ZAP-NRs and BeRST. No PL modulations were observed (Fig. S12a-c); Lastly, (vi) no significant PL changes were observed for non-specifically adsorbed ZAP-NRs to glass surfaces (Fig. S12d-f) upon [K^+] modulation, and no significant autofluorescence changes were observed for unlabeled live HEK293T cells upon [K^+] modulation (Fig. S12g-i). Photostability of ZAP-NRs labeled HEK cells was much stable than BeRST labeled HEK cells for 10 minutes under wide-field illumination under microscope. (Fig. S13)

The results shown in Fig. 4 and the series of control experiments suggest that the ΔF/F signal reports on membrane potential modulation at the ensemble level. Although the magnitude of ΔF/F is very small (~1%), this result is statistically significant, and quite surprising. Our small ΔF/F is much lower than other nanoparticle based voltage sensor's, such as a quasi-type II QDs in PMMA matrix placed between electrodes showing ~ΔF/F=2% per 20 mV under a synthetic voltage sweep.[9] Also, QD-C_{60} conjugates have been reported as a membrane potential nanosensor via electron transfer.[10] Their ΔF/F showed ~2% in stimulated cortical neurons in mouse cortex and ~20% in live cultured cells modulated between resting and depolarizing potentials. Even though the ΔF/F of ZAP NRs is very small (~1%), our voltage-sensitive NR showed reversible voltage-responsibility under periodic buffer exchange cycles. Moreover, our ZAP-NRs showed their PL turn-on in respond to depolarization, whereas these nanosensor's showed their PL was turned off.[9, 10] Possibly, this unique advantage of our ZAP NRs provide more sensitive voltage sensing and lower false-positive error rate from photo-darkening effect under electric field.

We previously demonstrated that quasi-type-II CdSe/CdS seeded NRs can report on membrane potential via the quantum confined Stark effect (QCSE) at the single

particle level and measured the QCSE for type-II ZnSe/CdS seeded NRs at the single particle level under *in vitro* conditions.[14, 15] In the later cases, single particle QCSE measurements exhibited slightly different distributions of positive (43%) and negative (57%) ΔF/F for randomly oriented type-II ZnSe/CdS seeded NRs. This slight asymmetry could possibly explain the small ΔF/F measured here on the ensemble level.

We also observed, in disagreement with QCSE predictions, positive correlation between spectral shifts (Δλ) and PL changes (ΔF/F) for type-II ZnSe/CdS seeded nanorods[14]. We hypothesized that extrinsic charging/ionization at surface- and interface-defects[27] could possibly modulate blinking rates (and hence QY) and contribute to the positive Δλ-ΔF/F correlation. Such contributions could add up at the ensemble level and therefore be responsible for the ensemble signal observed here. Further studies that correlate spectral, intensity and lifetime measurements under applied electric field and at different excitation powers are currently the topic of a follow-up project.

We have demonstrated QY modulation, at the ensemble level, of functionalized and membrane-targeted type-II ZnSe/CdS seeded nanorods for vesicles treated with valinomycin and for wild type HEK cells under alternating buffers with varying K^+ concentrations. ΔF/F of ~ 1% per 200 mV were achieved. Although the mechanism for these QY modulations is not confirmed as of yet (and is currently under investigation), it is likely not due to the QCSE. Regardless of the mechanism (QCSE or charging/quenching), voltage-sensing nanorods could possibly open up a new nano-neuroscience avenue for highly sensitivity, noise-immune action potential visualization across a large neural network.

Corresponding Author

*Corresponding author. E-mail: sweiss@chem.ucla.edu

Author contributions

J.P. conducted all experiments, analyzed all the data, and wrote the manuscript. J.P., Y.K., and J.L. synthesized ZnSe/CdS NRs using WANDA. Y.K. and J.P. developed the cell assay and built the flow setup. S.W., J.P., and Y.K. designed the experiments. S.W., E.M. and Y.K. helped in writing and revising the manuscript. All authors have given approval to the final version of the manuscript.

Competing interests: S.W., Y.K., and J.L. are inventors on a U.S. Provisional Patent application submitted by the University of California, Los Angeles (application no. 62504307, filed 05 October 2017). All other authors declare that they have no competing interests.

Acknowledgements:

We acknowledge Dr. H. Ronald Kaback for assisting with the chemically driven cell membrane modulation assay. We acknowledge Dr. Emory Chan for help with the WANDA instrument. We acknowledge the help of Antonino Ingargiola for processing data from the modulation assay. We also acknowledge the use of instruments at the Electron Imaging Center for NanoMachines supported by the NIH (1S10RR23057 and GM071940 to Z.H.Z.) and the Advanced Light Microscopy/Spectroscopy core, both at

the California NanoSystems Institute in the University of California, Los Angeles. Lastly, we acknowledge the participation in the USER Program (#1726 and #3244) of the Molecular Foundry at the Lawrence Berkeley National Laboratory, which was supported by the U.S. Department of Energy Office of Science, Office of Basic Energy Sciences under contract no. DE-AC02-05CH11231. S.W. acknowledges funding from the United States–Israel Binational Science Foundation (#2010382), the Human Frontier Science Program (#RGP0061/2015), the Defense Advanced Research Projects Agency/ Biological Technologies Office award no. #D14PC00141, the European Research Council (ERC) advanced grant NVS #669941, and the BER program of the Department of Energy Office of Science, grant # DE-FC03-02ER63421. This work was also supported by STROBE: A National Science Foundation Science & Technology Center under Grant No. DMR 1548924."

Supporting Information Available: Infrared spectrum of type-II ZnSe/CdS nanorod samples, zeta potential and dynamic light scattering plot of NRs, flow cytometry data of ZAP NRs labeled HEK cells, wide-field microscope image of ZAP NRs labeled giant unilamellar vesicle, photoluminescence spectrum of ZAP NRs labeled vesicles, $\Delta F(t)/F$ plot and threshold mask image of both BeRST dye and ZAP NRs labeled HEK cells under 7 cycles of chemical modulation, control experiments for chemical modulation in HEK cell membrane potential, *in-vitro* photoluminescence measurements in various $[K^+]$ and pH range, photostability plot of both BeRST dye and ZAP NRs labeled cells.

Materials and Methods

Materials: All chemicals are used as purchased without further purification. Trioctylphosphine oxide (TOPO, 99%), Octadecylphosphonic acid (ODPA) and hexylphosphonic acid (HPA) were purchased from PCI Synthesis. Tri-n-octylphosphine (TOP, 97%) was obtained from Strem Chemicals. Cadmium oxide (CdO), octadecylamine (ODA), hexadecylamine (HDA), octadecanethiol (ODT), 1.0 M diethylzinc ($Zn(Et)_2$) solution in hexanes, trimethyloxonium tetrafluoroborate (>95%), potassium chloride (KCl), (±)-alpha-lipoic acid (99%), N,N-dimehtylethylenediamine (>98%), 1,3-propanesultone (>98%), tris(2-carboxyethyl)phosphine (TCEP) hydrochloride, anhydrous chloroform, tetramethylammonium hydroxide solution (25% in methanol), dimethyl sulfoxide, and valinomycin (>97%) were purchased from Sigma-Aldrich. Selenium powder (99.999%, 200 mesh) was purchased from Alfa aesar. Di-8-anepps (D3167), DiR membrane labeling dye (D12731), Phenol-free DMEM, fetal bovine serum, penicillin/streptomycin, and trypsin solution were purchased from Thermo Fisher Scientific. The CG25 peptides were purchased from LifeTein. DOTAP (10 mg/mL in chloroform), DMPC (25 mg/mL in chloroform), and DC-cholesterol (10 mg/mL in chloroform) were purchased from Avanti Polar Lipids.

Preparation of ZnSe/CdS type-II nanorods

The procedure for synthesis of ZnSe quantum dots was adopted from a previous work.[17] Briefly, a mixture of Se (63 mg), TOP (2 g) and diethyl zinc solution (0.8 ml, 1 M) was injected into degassed HDA (7 g) at 300 ^{o}C in argon atmosphere. The reaction was kept at 265 ^{o}C until the desired absorption peak at 360 nm was observed (~30 mins after injection). After the flask was cooled to room temperature, ZnSe quantum dots were purified 3 times by butanol/methanol precipitation and redispersed in toluene. The

concentration of ZnSe in toluene was documented by the optical density (OD) at the absorption peak through a 1 cm cuvette.

ZnSe seeded CdS nanorods were synthesized using WANDA.[28] CdO (270 mg), ODPA (1305 mg), HPA (360 mg), and TOPO (13.5 g) were first degassed at 100 ^{o}C under vacuum for 2 hrs. The mixture was heated to 230 ^{o}C under nitrogen blanket until CdO powder was dissolved and a colorless solution was obtained. The solution was cooled down to 100 ^{o}C, ODA was added (180 mg), and the solution was degassed under vacuum for additional 2 hrs. To prepare the S precursor solution with ZnSe, 1440 mg of ODT were mixed with 36 units [OD (under 1cm path length) × ml] of ZnSe solution in toluene and degassed 100 ^{o}C under vacuum to remove the toluene and moisture. After degassing, both Cd precursor solution and S precursor with ZnSe were transferred under vacuum into a glove box and dispensed gravimetrically into the 40 ml glass vials used as reaction vessels for the robot. The filled vials were loaded into the eight-reactor array of WANDA, an automated nanocrystal synthesis robot at the Molecular Foundry. WANDA was used to run up to eight reactions in serial with individually controlled heating/cooling profiles, stirring rate, injections and aliquot schedules. Below is the description of an exemplary run. 1.133 ml of S/ZnSe solution (heated to 50 ℃ to prevent solidification) was injected into 15.615 g of Cd solution at 330 ℃ at a dispense rate of 1.5 ml/sec. The temperature after injection was set at 320 ℃ for CdS NR growth. The heating was stopped 15 mins after injection. To thermally quench the reaction, each reaction was then rapidly cooled to 50℃ using a stream of nitrogen, after which 5 ml of acetone was injected.

Functionalization of NRs by zwitterionic decorated lipoic acids (zw-LA) and alpha-helical peptides

100 mg of as synthesized NRs were mixed with 0.5 mL of stripping agent solution (0.1 M trimethyloxonium tetrafluoroborate in hexane) and the solution was heated to 55 ^{o}C for 5 minutes. It was then spun down (10,000 rcf, 2 minutes) and the clear supernatant solution containing the NRs was recovered. Next, the solvent was completely removed by vacuum at 50 ^{o}C. 0.5 mL of octanoic acid was added to the dried NRs and sonicated for 5 minutes. 0.1 mL of methanol was added to the NRs solution and the mixture was spun down (10,000 rcf, 2 minutes). The NRs' precipitate was redispersed in 0.5 mL of pyridine. 0.2 mL of hexane was added to the NRs solution and spun down (10,000 rcf, 2 minutes). The NRs were then redispersed in 0.5 mL of pyridine. The extinction coefficient of the NRs was determined by ICP-AES measurement to be $\varepsilon = 8 \times 10^6$ L mol cm^{-1}. NRs' absorbance at 400 nm (in pyridine) was used to construct a concentration calibration curve. For the preparation of 3 μM NRs stock solution, 0.1 nmol NRs in 1 mL pyridine solution was placed in glass vial. 3 μmol of the alpha helical peptides (CG25, sequence: C_{13}(myristoyl)-CLTCALTCMECTLKCWYKRGCRGCG-carboxylate) in 1.8 mL DMSO and 10 μL of the zwitterionic decorated lipoic acids (zw-LA)[18] (from 0.1 M stock solution in DI water), which were reduced by adding 40 μL of tris(2-carboxyethyl)phosphine (TCEP, 0.5 M stock solution in DI water, pH 7.0)) to the solution. The reduced peptides / zw-LA mixture was added to the NRs solution in pyridine and vigorously stirred for 10 minutes. 5 μL of 5% tetramethylammonium hydroxide (TMAOH) solution in methanol was then added to the crude NR solution and the mixture was then spun down (10,000 rcf, 2 minutes). The precipitate of NRs was redispersed in 33 μL DMSO and to yield 3 μM of functionalized NRs solution. NRs' QY was determined by comparison to the known QY of the reference rhodamine 101 (Rhodamine 640) dye in methanol (100%). BeRST's QY was determined by comparison to the known QY of

the reference cresyl violet in methanol (54%). PL spectrum of the sample was measured by PTI QuantaMaster spectrofluorometer (HORIBA).

Cell Culture

HEK293T cells (human embryonic kidney cell line) were maintained in DMEM media (GIBCO) supplemented with 10% (v/v) fetal bovine serum (FBS) and 1% (v/v) penicillin/streptomycin (growth media) for cell adhesion. Culture media was replaced 24 hours prior to imaging and $[K^+]$ modulation experiments with phenol red-free DMEM media supplemented with 10% (v/v) fetal bovine serum (FBS) and 1% (v/v) penicillin/streptomycin (imaging media)

Membrane loading of ZAP-NRs for $[K^+]$ modulation experiments

Cultured HEK293T cells (~5,000 cells per channel, 6-channels µ-slide chamber, ibidi) were co-incubated with 5 µM valinomycin for 5 minutes at 37ºC. Excess amount of valinomycin was removed by washing 3 times with phenol red-free DMEM media. 30 nM of ZAP-NRs were directly added in the DMEM media and incubated for 15 minutes at room temperature. For dual labeled with BeRST dye, 200 nM of BeRST in DMSO was incubated for 15 minutes sequentially. Control samples were identically prepared skipping the valinomycin loading step. For fixation, cells were incubated in 4% paraformaldehyde (in 0.01M PBS buffer, pH 7.4) for 10 minutes at room temperature and washed twice with 0.01M PBS buffer. For $[K^+]$ modulation experiments, two reservoirs containing $[K^+]$=140 mM KCl and $[K^+]$=2.7 mM KCl with 274.6 mM sucrose in HEPES buffer (20 mM, pH 7.4) were connected to a single inlet tube (via a T-connector) of the flow chamber and controlled via computer-controlled valves. The constant flow rate (5

mL/min) was controlled by peristaltic pump. The outlet of the chamber was connected via another single tube to the waste reservoir. A home-written Labview code controlled the valves via a USB DAQ (USB-6001, National Instruments) and provided a trigger signal to the EMCCD (Ixon EM^+ EMCCD, Andor). An 'ensemble level' $\Delta F(t)/F$ was calculated in the following way: An 'ensemble level' $\Delta F(t)/F$ was calculated from the movie in the following way: First, all pixels above a threshold (Fig S9) per single frame were averaged. This quantity was then averaged over all frames (time points) to yield F. Next, $\Delta F(t)$ was defined as the difference between the averaged intensity over all pixels for a single frame (for each time point) and F.

Optical imaging

For dual-view setup in chemical modulation assay using two different potassium buffers, The microscope setup was based on a Nikon Ti inverted microscope equipped with LED light source (Aura, Lumencor) and excitation filter (ET470/40x, Chroma Technology Corp). The emissions of the NRs and BeRST dye were collected by x60 oil immersion, 1.4 NA objective was used for all imaging experiments. A 530 nm LP emission filter filter (E530LP, Chroma Technology Corp) and multiband dichroic mirror (FF545/650-Di01, Semrock) were used to block the LED excitation and pass the emission to the dual-view Optosplit unit (Optosplit II, Cairn Research) which was mounted in front of Andor iXon EMCCD camera (Andor iXon EM^+, Andor). The optosplit was configured with a 640 nm dichroic (FF640-FDi01, Semrock) and 700 nm LP filters (FELH0700, Thorlab) for the BeRST channel, and with 585/40 bandpass filter (FF01-585/40, Semrock) for ZAP-NRs channel. The excitation intensity was adjusted to 0.2 mW/cm^2 in front of the objective lens. The frame rate was 10 Hz. Wide-field fluorescence images of ZAP-NRs labeled

cells were acquired with a Nikon Ti inverted microscope equipped with LED light source (Aura, Lumencor) and TxRed filter cube (BP 560/40 for excitation, 595DC, BP 630/60 for emission). Images were recorded with an Ador iXon EMCCD camera (Andor iXon EM^+, Andor).

Co-localization by confocal microscopy

HEK293T cells were cultured in glass-bottom dishes (diameter: 35 mm; $3x10^5$ cells per dish) were incubated with 30 nM ZAP-NRs for 1 hour and with 2 µM DiR dye (D12731, Thermo Fisher Scientific) for 15 minutes at 37 ^oC, sequentially. Excess amounts of both the dyes and the NRs were removed by 3 successive washing steps with phenol red-free DMEM media. The cells were fixed with 4% paraformaldehyde (in 0.01M PBS buffer, pH 7.4) for 10 minutes at room temperature. Fixed cells were washed 3 times with PBS buffer (0.01 M, pH 7.4) and placed in phenol red-free DMEM media. Confocal images were recorded by an inverted Leica TCS-SP8-SMD Confocal Microscope at the CNSI's Advanced Light Microscopy/ Spectroscopy core facility.

DLS measurements

10 nM ZAP-NRs (as final concentration) samples were dispersed in 0.2, 1, 10 % DMSO (aq) solution. For control samples, 100% DMSO and DI water were used as solvents. The Wyatt DynaPro Plate Reader II (Wyatt Technology) was used to acquire DLS data and extract hydrodynamic radii of the samples.

GUVs preparation and ZAP-NRs loading for $[K^+]$ modulation experiments

Giant unilamellar vesicles (GUVs) were prepared according to the following

protocol: 6 µL of 1,2-dioleoyl-3-trimethylammonium-propane (chloride salt) (DOTAP, 10 mg/mL in chloroform), 6 µL of 1,2-dimyristoyl-sn-glycero-3-phosphocholine (DMPC, 25 mg/mL in chloroform), 6 µL of (3ß-[N-(N',N'-dimethylaminoethane)-carbamoyl]cholesterol hydrochloride, DC-cholesterol, 10 mg/mL in chloroform) were mixed in glass vial and chloroform was removed under vacuum at room temperature. 1 mL HEPES buffer (20 mM, pH 7.4) with KCl ($[K^+]$=140 mM) was added to the dried lipids in the glass vial and incubated at 37^{o}C for 24 hours. The vial was vigorously shaken and stored at 37^{o}C for 24 hours to form GUVs. For ZAP-NRs labeling, 1 µL of ZAP NRs stock solution (3 µM) were treated to the GUVs and incubated for 5 minutes. To build up the membrane potential, the 1 uL of GUV solution was diluted in 1 mL HEPES buffer (20 mM, pH 7.4) with KCl ($[K^+]$=2.7 mM with with 274.6 mM sucrose) Valinomycin was added after 60 seconds from the starting time for acquiring PL data of ZAP NRs loaded GUVs. Time-lapse PL intensity of each sample for 120 seconds at ZAP NRs peak wave length (605 nm) was measured by PTI QuantaMaster spectrofluorometer (HORIBA).

In-vitro PL measurements of ZAP-NRs as function of $[K^+]$ and pH

PL measurements of ZAP-NRs as function of $[K^+]$: 300 nM of ZAP-NRs were placed in 0, 0.5, 1, 2, 5, 10, 20, 50, 100, and 200 mM of potassium chloride contained HEPES buffer. To maintain constant ionic strength, 400, 399, 398, 396, 390, 380, 360, 300, 200, and 0 mM of sucrose were dissolved and added to each HEPES buffer, respectively. PL spectrum of each sample was measured by PTI QuantaMaster spectrofluorometer (HORIBA).

PL measurements of ZAP-NRs as function of pH: 300 nM of ZAP-NRs were

placed in pH 4, 6, 7.4, 8, 10 buffer (for pH 4; 50 mM acetate buffer, for pH 6, 7.4; 50 mM MES buffer, for pH 8, 10; 50 mM PBS buffer). PL spectrum of each sample was measured by PTI QuantaMaster spectrofluorometer (HORIBA).

Flow cytometry analysis

To investigate the labeling efficiency of ZAP NRs, HEK293T cells were cultured and they were co-incubated with the ZAP NRs. The cells were grown in DMEM growth media for cell adhesion. To optimize the labeling efficiency of ZAP NRs, 5×10^4 HEK293T cells were co-cultured with the 30 nM of ZAP NRs for 15 minutes, 30, 45, 60, 90, or 120 minutes in phenol red-free DMEM media. The cells were detached by adding a 0.25% trypsin and EDTA solution. The cells were then rinsed with PBS buffer (0.1 M, pH 7.4) with 1% FBS (FACS buffer) for three times and re-dispersed in fixing buffer (1% formaldehyde in FACS buffer). The collected cells were further analyzed with flow cytometry.

References

1. Wu, J. Y.; Cohen, L. B.; Falk, C. X. Neuronal Activity during Different Behaviors in Aplysia: A Distributed Organization? *Science* **1994,** *263*, 820.
2. Grinvald, A.; Hildesheim, R. VSDI: a new era in functional imaging of cortical dynamics. *Nat. Rev. Neurosci.* **2004,** *5*, 874-885.
3. Peterka, D. S.; Takahashi, H.; Yuste, R. Imaging Voltage in Neurons. *Neuron 69*, 9-21.
4. Preuss, S.; Stein, W. Comparison of Two Voltage-Sensitive Dyes and Their Suitability for Long-Term Imaging of Neuronal Activity. *PLoS ONE* **2013,** *8*, e75678.
5. St-Pierre, F.; Marshall, J. D.; Yang, Y.; Gong, Y.; Schnitzer, M. J.; Lin, M. Z. High-fidelity Optical Reporting of Neuronal Electrical Activity with An Ultrafast Fluorescent Voltage Sensor. *Nat. Neurosci.* **2014,** *17*, 884

6. Gong, Y.; Huang, C.; Li, J. Z.; Grewe, B. F.; Zhang, Y.; Eismann, S.; Schnitzer, M. J. High-speed Recording of Neural Spikes in Awake Mice and Flies with a Fluorescent Voltage Sensor. *Science* **2015,** *350*, 1361.
7. Kannan, M.; Vasan, G.; Huang, C.; Haziza, S.; Li, J. Z.; Inan, H.; Schnitzer, M. J.; Pieribone, V. A. Fast, in vivo Voltage Imaging Using a Red Fluorescent Indicator. *Nat. Methods* **2018,** *15* (12), 1108-1116.
8. Abdelfattah, A. S.; Kawashima, T.; Singh, A.; Novak, O.; Liu, H.; Shuai, Y.; Huang, Y.-C.; Grimm, J. B.; Patel, R.; Friedrich, J.; et al. Bright and Photostable Chemigenetic Indicators for Extended in vivo Voltage Imaging. *bioRxiv* **2018**, 436840.
9. Rowland, C. E.; Susumu, K.; Stewart, M. H.; Oh, E.; Mäkinen, A. J.; O'Shaughnessy, T. J.; Kushto, G.; Wolak, M. A.; Erickson, J. S.; L. Efros, A.; et al. Electric Field Modulation of Semiconductor Quantum Dot Photoluminescence: Insights Into the Design of Robust Voltage-Sensitive Cellular Imaging Probes. *Nano Lett.* **2015,** *15*, 6848-6854.
10. Nag, O. K.; Stewart, M. H.; Deschamps, J. R.; Susumu, K.; Oh, E.; Tsytsarev, V.; Tang, Q.; Efros, A. L.; Vaxenburg, R.; Black, B. J.; et al. Quantum Dot–Peptide–Fullerene Bioconjugates for Visualization of in Vitro and in Vivo Cellular Membrane Potential. *ACS Nano* **2017,** *11*, 5598-5613.
11. Park, K.; Deutsch, Z.; Li, J. J.; Oron, D.; Weiss, S. Single Molecule Quantum-Confined Stark Effect Measurements of Semiconductor Nanoparticles at Room Temperature. *ACS Nano* **2012,** *6*, 10013-10023.
12. Park, K.; Weiss, S. Design Rules for Membrane-Embedded Voltage-Sensing Nanoparticles. *Biophys. J.* **2017,** *112*, 703-713.
13. Park, K.; Kuo, Y.; Shvadchak, V.; Ingargiola, A.; Dai, X.; Hsiung, L.; Kim, W.; Zhou, H.; Zou, P.; Levine, A. J.; et al. Membrane insertion of—and membrane potential sensing by—semiconductor voltage nanosensors: Feasibility demonstration. *Sci. Adv.* **2018,** *4*. e1601453
14. Kuo, Y.; Li, J.; Michalet, X.; Chizhik, A.; Meir, N.; Bar-Elli, O.; Chan, E.; Oron, D.; Enderlein, J.; Weiss, S. Characterizing the Quantum-Confined Stark Effect in Semiconductor Quantum Dots and Nanorods for Single-Molecule Electrophysiology. *ACS Photonics* **2018**, *5*, 4788-4800
15. Bar-Elli, O.; Steinitz, D.; Yang, G.; Tenne, R.; Ludwig, A.; Kuo, Y.; Triller, A.; Weiss, S.; Oron, D. Rapid Voltage Sensing with Single Nanorods via the Quantum Confined Stark Effect. *ACS Photonics* **2018,** *5*, 2860-2867.
16. Efros, A. L.; Delehanty, J. B.; Huston, A. L.; Medintz, I. L.; Barbic, M.; Harris, T. D. Evaluating the Potential of Using Quantum Dots for Monitoring Electrical Signals in Neurons. *Nat. Nanotechnol.* **2018,** *13*, 278-288.
17. Dorfs, D.; Salant, A.; Popov, I.; Banin, U. ZnSe Quantum Dots Within CdS Nanorods: A Seeded-Growth Type-II System. *Small* **2008,** *4*, 1319-1323.
18. Park, J.; Nam, J.; Won, N.; Jin, H.; Jung, S.; Jung, S.; Cho, S.-H.; Kim, S. Compact and Stable Quantum Dots with Positive, Negative, or Zwitterionic Surface: Specific Cell Interactions and Non-Specific Adsorptions by the Surface Charges. *Adv. Funct. Mater.* **2011,** *21*, 1558-1566.
19. Rosen, E. L.; Buonsanti, R.; Llordes, A.; Sawvel, A. M.; Milliron, D. J.; Helms, B. A. Exceptionally Mild Reactive Stripping of Native Ligands from Nanocrystal Surfaces by Using Meerwein's Salt. *Angew. Chem. Int. Ed.* **2012,** *51*, 684-689.

20. Montana, V.; Farkas, D. L.; Loew, L. M. Dual-wavelength Ratiometric Fluorescence Measurements of Membrane Potential. *Biochemistry* **1989,** *28*, 4536-4539.
21. Bifano, E. M.; Novak, T. S.; Freedman, J. C. Relationship between the Shape and the Membrane Potential of Human Red Blood Cells. *J. Membr. Biol.* **1984,** *82*, 1-13
22. Kao, L.; Azimov, R.; Shao, X. M.; Frausto, R. F.; Abuladze, N.; Newman, D.; Aldave, A. J.; Kurtz, I. Multifunctional Ion Transport Properties of Human SLC4A11: Comparison of the SLC4A11-B and SLC4A11-C Variants. *Am. J. Physiol. Cell Physiol.* **2016,** *311*, C820-C830.
23. Huang, Y.-L.; Walker, A. S.; Miller, E. W. A Photostable Silicon Rhodamine Platform for Optical Voltage Sensing. *J. Am. Chem. Soc.* **2015,** *137*, 10767-10776.
24. DiFranco, M.; Capote, J.; Vergara, J. L. Optical Imaging and Functional Characterization of the Transverse Tubular System of Mammalian Muscle Fibers using the Potentiometric Indicator di-8-ANEPPS. *J. Membr. Biol.* **2005,** *208*, 141-153.
25. Kao, W. Y.; Davis, C. E.; Kim, Y. I.; Beach, J. M. Fluorescence Emission Spectral Shift Measurements of Membrane Potential in Single Cells. *Biophys. J.* **2001,** *81*, 1163-1170.
26. Manno, C.; Figueroa, L.; Fitts, R.; Ríos, E. Confocal Imaging of Transmembrane Voltage by SEER of di-8-ANEPPS. *J. Gen. Physiol.* **2013,** *141*, 371-387.
27. Park, S.-J.; Link, S.; Miller, W. L.; Gesquiere, A.; Barbara, P. F. Effect of Electric Field on the Photoluminescence Intensity of Single CdSe Nanocrystals. *Chem. Phys.* **2007,** *341*, 169-174.
28. Chan, E. M.; Xu, C.; Mao, A. W.; Han, G.; Owen, J. S.; Cohen, B. E.; Milliron, D. J. Reproducible, High-Throughput Synthesis of Colloidal Nanocrystals for Optimization in Multidimensional Parameter Space. *Nano Lett.* **2010,** *10*, 1874-1885.